

Mathematical Sciences Exercise Answer Part I

Baiyuan Chen *

The University of Tokyo

Contents

1 Nonlinear Dynamical Systems	2
1.0 Numerical Integration Methods for Ordinary Differential Equations	2
1.0.0 Exercise 1.0.0	2
1.1 Linear Stability Analysis and Nonlinear Oscillations	2
1.1.1 Exercise 1.1.1	2
1.1.2 Exercise 1.1.2	5
1.2 Synchronization Phenomenon in Nonlinear Oscillators	9
1.2.0 Exercise 1.2.0	9
1.3 Neuron Excitation Phenomenon and Hodgkin-Huxley Equations	14
1.3.1 Exercise 1.3.1	14
1.4 Chaos	19
1.4.0 Exercise 1.4.0	19
1.4.1 Exercise 1.4.1	24

*Email: chenbaiyuan75@gmail.com

1 Nonlinear Dynamical Systems

1.0 Numerical Integration Methods for Ordinary Differential Equations

1.0.0 Exercise 1.0.0

Numerically solve the following harmonic oscillator using the Euler method and the 4th-order Runge-Kutta method.

$$\frac{d^2x}{dt^2} = -x \quad (1)$$

Change the step size and compare how the phase space trajectories differ for each method. Also, verify how the value of $x^2 + (\frac{dx}{dt})^2$ changes over time.

The phase space trajectories solved using the Euler method and the 4th-order Runge-Kutta method are shown below (Fig. 1).

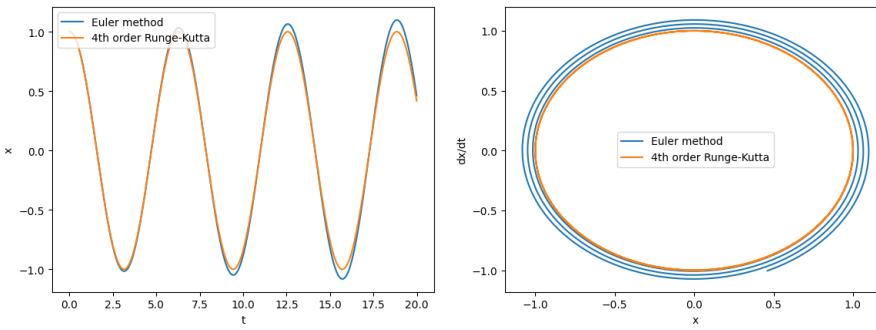


Figure 1: Time evolution of x (left) and the phase space of x and $\frac{dx}{dt}$ (right)

The change in the value of $x^2 + (\frac{dx}{dt})^2$ over time is shown in Fig. 2.

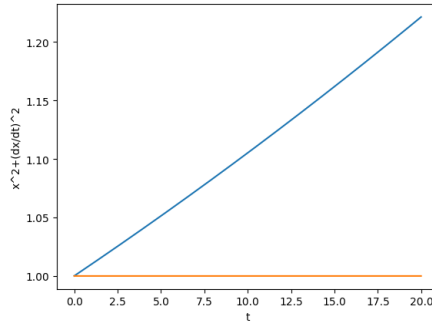


Figure 2: Time evolution of the value of $x^2 + (\frac{dx}{dt})^2$

1.1 Linear Stability Analysis and Nonlinear Oscillations

1.1.1 Exercise 1.1.1

$$\frac{d^2x}{dt^2} - (A + D)\frac{dx}{dt} + (AD - BC)x = 0. \quad (2)$$

1. Organize the conditions for each of the 6 fixed points obtained for the parameters A, B, C, and D in the differential equation above.

The characteristic equation of Eq. (2)

$$\lambda^2 - (A + D)\lambda + (AD - BC) = 0 \quad (3)$$

indicates that the fixed points are:

- Stable focus when $(A - D)^2 + 4BC < 0, A + D < 0,$
- Unstable focus when $(A - D)^2 + 4BC < 0, A + D > 0,$
- Center when $(A - D)^2 + 4BC < 0, A + D = 0,$
- Stable node when $(A - D)^2 + 4BC > 0, A + D < 0,$
- Unstable node when $(A - D)^2 + 4BC > 0, A + D > 0,$
- Saddle point when $A + D + \sqrt{(A - D)^2 + 4BC} > 0 > A + D - \sqrt{(A - D)^2 + 4BC}.$

2. Construct differential equations for each condition, solve them numerically using a computer, and plot the phase space trajectories.

Stable spiral: $A=1, B=1, C=-3, D=-2.$

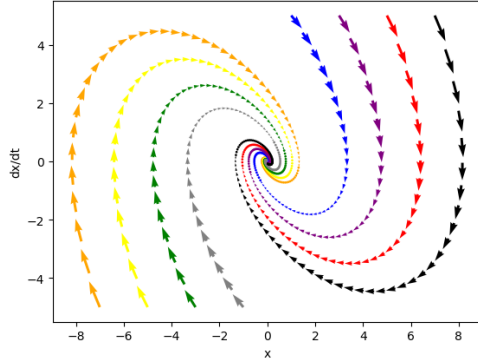


Figure 3: Stable focus

Unstable spiral: $A=2, B=1, C=-3, D=-1.$

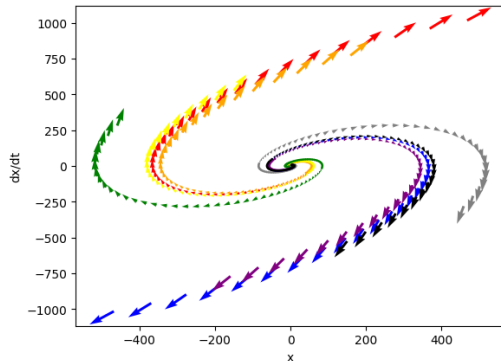


Figure 4: Unstable focus

Center: $A=1, B=1, C=-3, D=-1.$

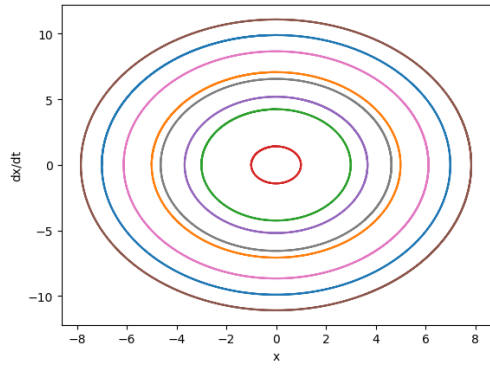


Figure 5: Center

Stable node: $A=-3, B=0, C=0, D=-1$.

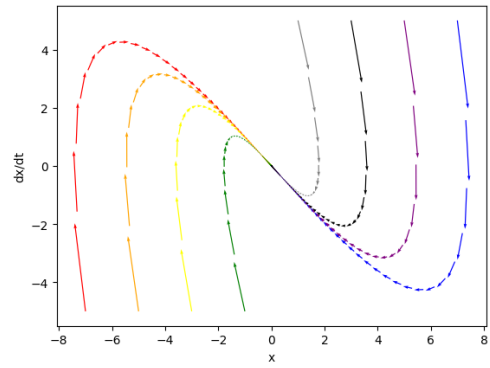


Figure 6: Stable node

Unstable node: $A=1, B=1, C=-4, D=5$.

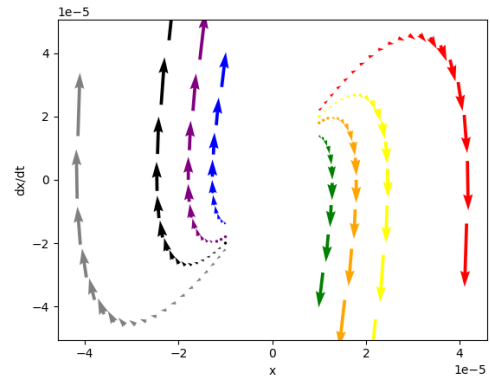


Figure 7: Unstable node

Saddle point: $A=-1, B=2, C=2, D=2$.

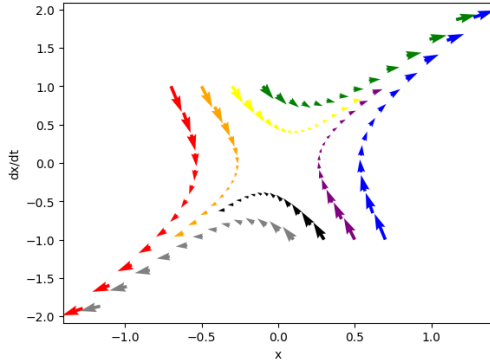


Figure 8: Saddle point

3. Classify the harmonic and damped oscillators.

The fixed point of the harmonic oscillator is the center, while the damped oscillator has a stable focus.

1.1.2 Exercise 1.1.2

van der Pol equation:

$$\frac{d^2x}{dt^2} - \mu(1-x^2)\frac{dx}{dt} + x = 0 \quad (\mu > 0) \quad (4)$$

After a change of variables, this equation becomes Eq. (5).

$$\frac{d^2x}{dt^2} - (\epsilon - x^2)\frac{dx}{dt} + x = 0 \quad (\epsilon > 0) \quad (5)$$

1. Perform linear stability analysis and examine the stability of fixed points.

When $\epsilon > 0$, the time to reach stability becomes longer as ϵ approaches 0. It is an unstable node when $\epsilon > 2$, and an unstable focus when $0 < \epsilon < 2$.

At $\epsilon = 0$, it is a center.

When $\epsilon < 0$, the time to reach stability becomes longer as ϵ approaches 0. It is a stable focus when $0 > \epsilon > -2$ and a stable node when $\epsilon < -2$.

2. Solve the equation using a computer. Plot the time evolution and the solution trajectories in the phase space. Observe the behavior of trajectories starting from various initial conditions. How does the qualitative behavior of the solution change with different values of ϵ ?

When $\epsilon > 2$, it is an unstable node.

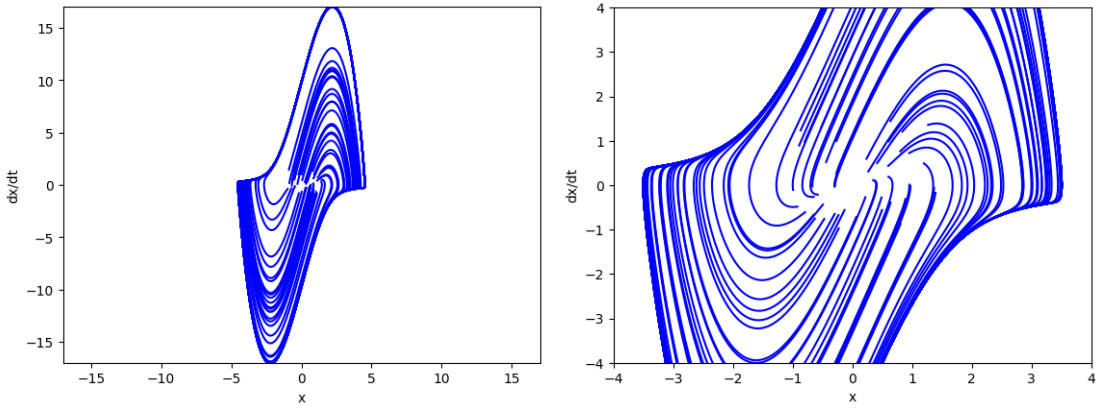


Figure 9: $\epsilon = 5$ (left), 3 (right)

When $0 < \epsilon < 2$, it is an unstable focus. The solution is not stable when $\epsilon > 0$, and the width of the solution trajectory becomes smaller as ϵ approaches 0.

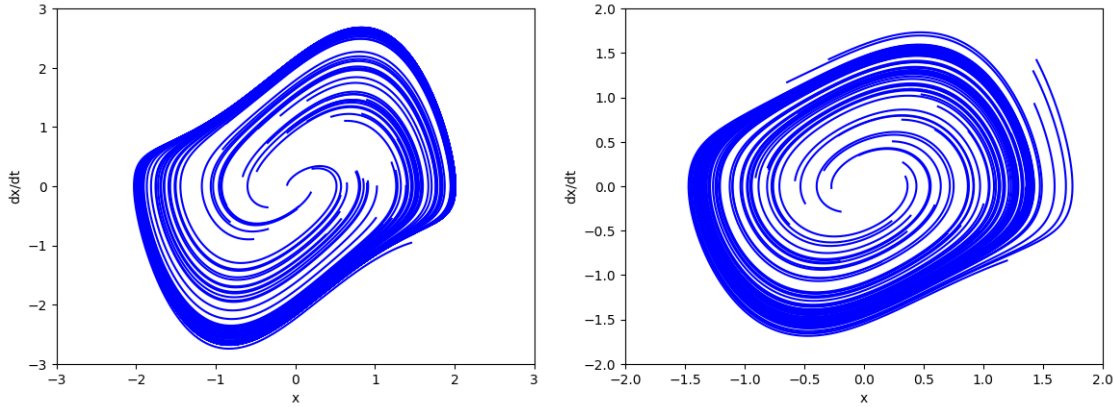


Figure 10: $\epsilon = 1$ (left), 0.5 (right)

When $\epsilon = 0$, it is a center.

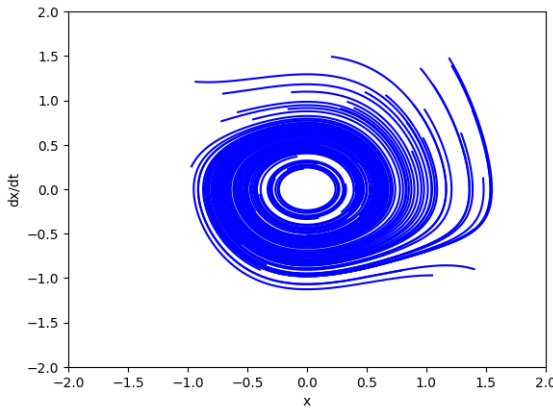


Figure 11: Center

When $0 > \epsilon > -2$, it is a stable focus.

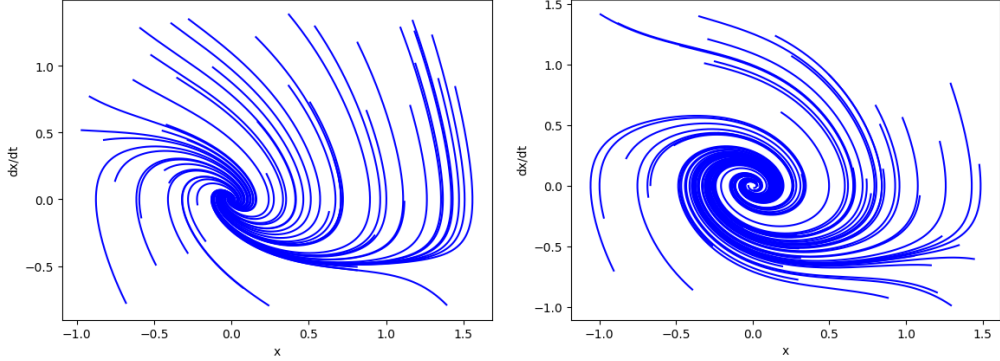


Figure 12: $\epsilon = -1$ (left), -0.5 (right)

When $\epsilon < -2$, it is a stable node. For $\epsilon < 0$, the solution becomes stable, and the time to reach stability becomes longer as ϵ approaches 0.

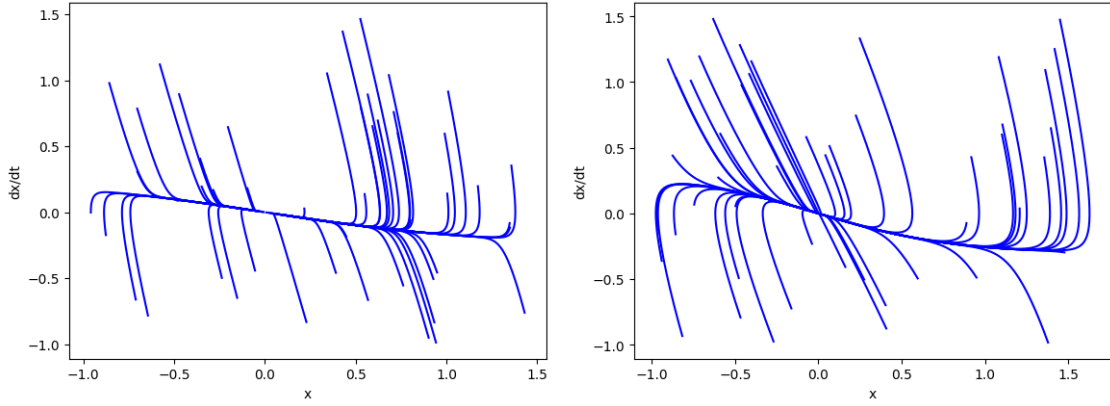


Figure 13: $\epsilon = -5$ (left), -3 (right)

3. Take the Poincaré section at $\dot{x} = 0$ and observe the trajectory behavior for various initial conditions.

In Figs. (14)-(16) left, the behavior of the trajectory on the Poincaré section at $\dot{x} = 0$ is shown in Figs. (14)-(16) right. When $\epsilon = -0.5$, it is a stable focus, so the value of x at $\dot{x} = 0$ becomes stable quickly. In contrast, when $\epsilon > 0$, the solution is unstable, and eventually, the value of x at $\dot{x} = 0$ alternates between a certain value and its opposite.

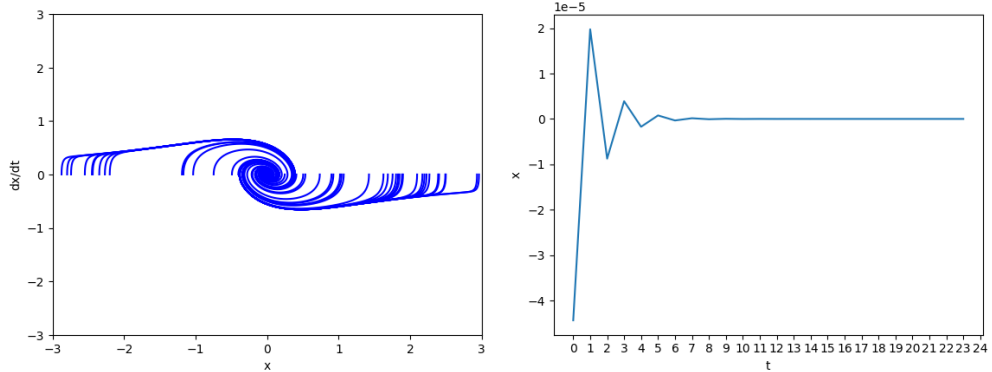


Figure 14: Poincaré section at $\dot{x} = 0$ ($\epsilon = -0.5$)

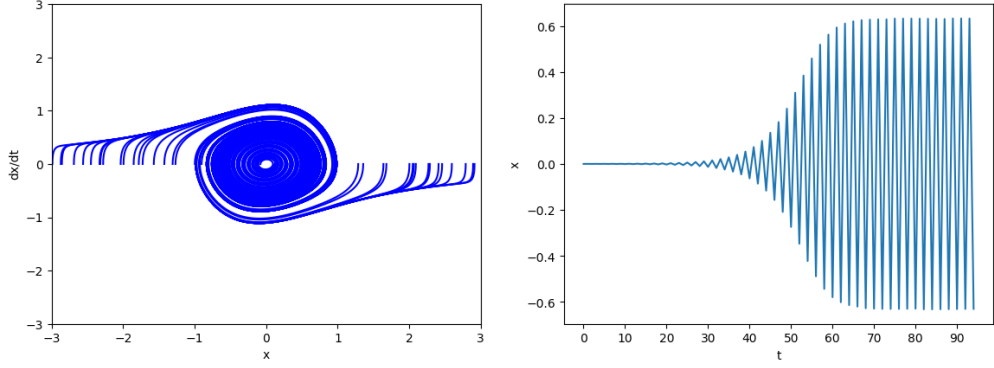


Figure 15: Poincaré section at $\dot{x} = 0$ ($\epsilon = 0.1$)

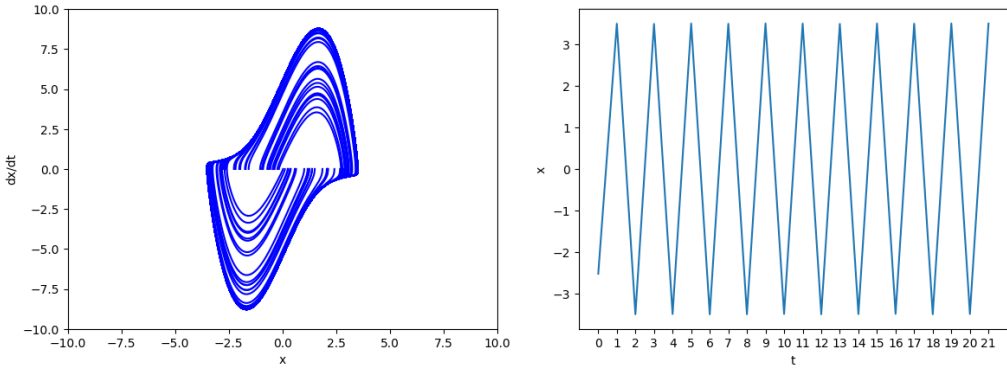


Figure 16: Poincaré section at $\dot{x} = 0$ ($\epsilon = 3$)

4. The discretized trajectory on the Poincaré section (Poincaré map) is represented as $x_1, x_2, \dots, x_n, \dots$. Plot x_n on the horizontal axis and x_{n+1} on the vertical axis (return map), and observe the shape of the function as well as the asymptotic behavior of x_n as $n \rightarrow \infty$ for various initial conditions. Consider what this asymptotic state corresponds to and numerically explain the linear stability and uniqueness of this state.

As $n \rightarrow \infty$, the behavior of x_n approaches the line $x_{n+1} = x_n$, indicating that x_n is stable and has a unique value.

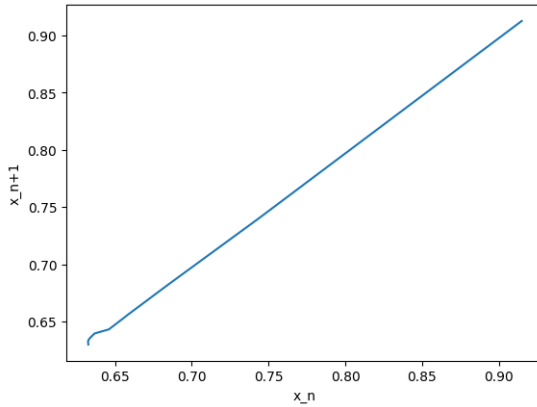


Figure 17: Return map of x_n ($\epsilon = 0.1$)

5. When ϵ is sufficiently small, how does the amplitude of the limit cycle depend on the parameter? Evaluate the order with respect to ϵ . Also, analytically explain this dependency.

The relationship between the amplitude of the limit cycle and ϵ is shown in Fig. (18). Fig. (19) illustrates the relationship between the logarithms of the limit cycle amplitude and ϵ . The slope is 0.5, indicating that the relationship between the limit cycle amplitude h and ϵ is $h = \epsilon^{\frac{1}{2}}$.

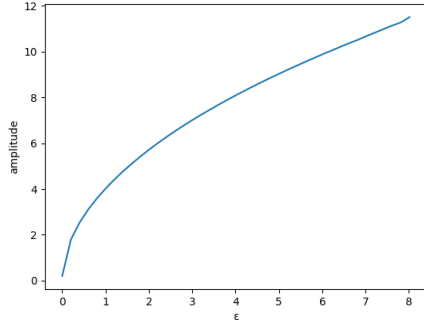


Figure 18: Relationship between the limit cycle amplitude and ϵ

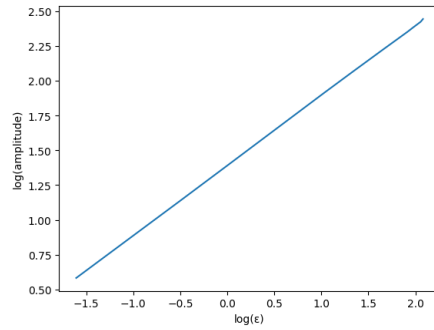


Figure 19: Logarithmic relationship between the limit cycle amplitude and ϵ

1.2 Synchronization Phenomenon in Nonlinear Oscillators

1.2.0 Exercise 1.2.0

1. For an appropriate value of μ , observe the behavior when varying F and ω . When $\mu = 1$, the behavior with different values of F and ω is shown in Fig. (20).

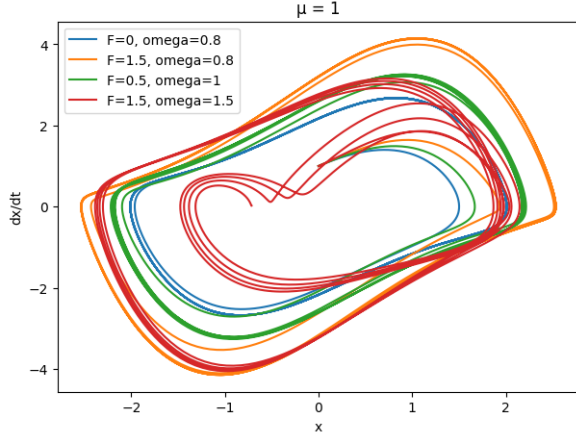


Figure 20: Behavior for different F and ω at $\mu = 1$

2. Characterize synchronization by the relative period of the limit cycle to the external force. For an appropriate value of F , observe the change in the relative period of the limit cycle with respect to ω .

When $F = 1$, the change in the relative period of the limit cycle with respect to ω is shown in Fig. (21). At $\omega = 0.8$, the relative period still changes, but it becomes constant at $\omega = 1$ and 1.5 .

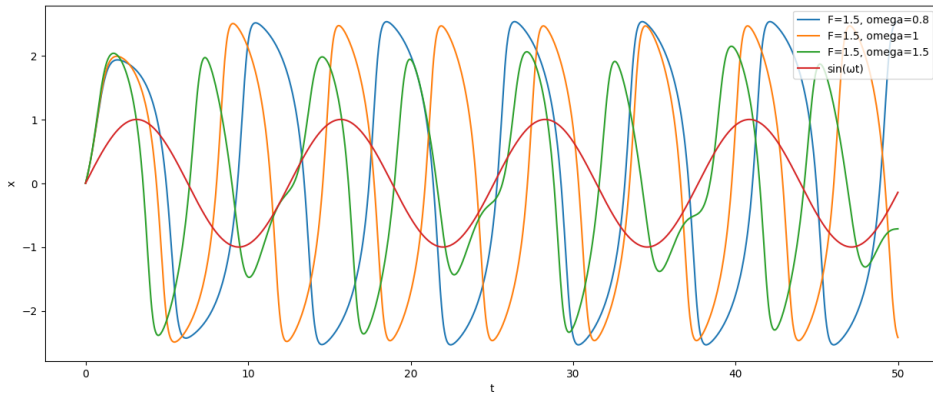


Figure 21: Change in the relative period of the limit cycle with respect to ω at $F = 1$

3. Plot a phase diagram with ω on the horizontal axis and F on the vertical axis, representing the parameter region where synchronization occurs (observe Arnold tongues).

At $\mu = 1$, the parameter region where synchronization occurs is shown by the inverted triangular region in Fig. (22).

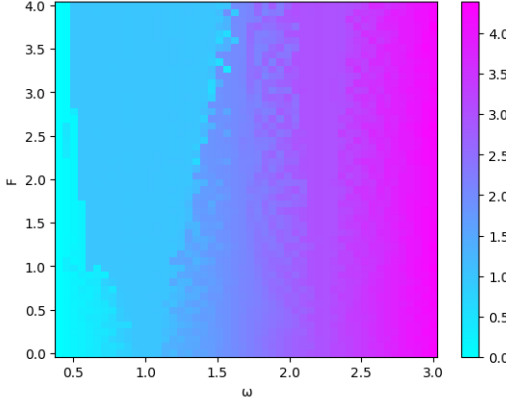


Figure 22: Phase diagram of ω and F

4. Observe how the dependency on F and ω changes with μ .

The dependency of F and ω when changing μ is shown in Fig. (23). As μ increases, the region where synchronization occurs in the phase diagram becomes narrower.

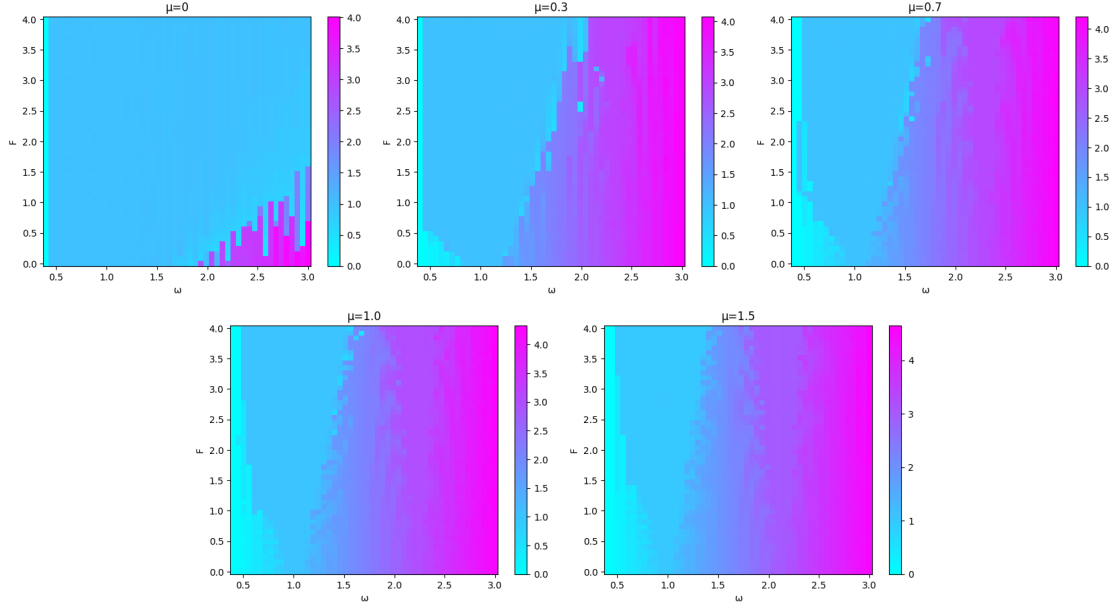


Figure 23: Dependency of F and ω at $\mu = 0, 0.3, 0.7, 1, 1.5$

5. Introducing the variable u defined by $\dot{u} = \omega$, the system becomes a 3-variable first-order differential equation. By setting $u(t + 2\pi/\omega) = u(t)$, forced synchronization can be regarded as motion on a T^2 torus. Take a Poincaré section on an appropriate u , observe the behavior of the solution, and construct a return map. Discuss the behavior of the attractor with respect to ω , and how this mapping corresponds to the solution trajectory on the torus.

The phase diagram for $\mu = 1$, $F = 1$, $\omega = 1.5$ is shown in Fig. (24) left. By introducing the variable u as described in the problem, taking the Poincaré section at $u = 0.5$ yields the solution trajectory shown in Fig. (24) right. This forced synchronization represents motion on a T^2 torus.

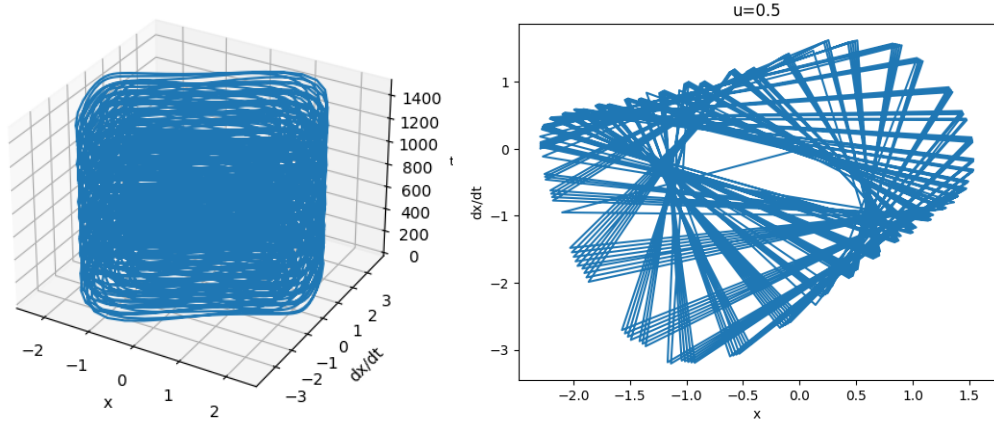


Figure 24: Phase diagram at $\mu = 1$, $F = 1$, $\omega = 1.5$ (left), Solution trajectory at $u = 0.5$ (right)

The return map at this point is shown in Fig. (25), which also represents motion on a T^2 torus.

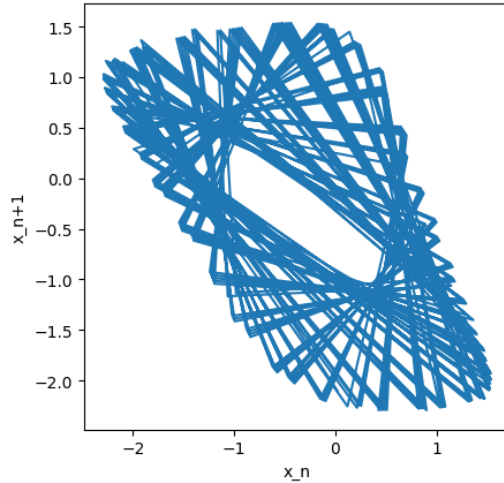


Figure 25: Return map

6. The synchronization phenomenon of oscillators can be modeled by the following 1-dimensional map:

$$\theta_{n+1} = \theta_n + \Omega - \left(\frac{K}{2\pi} \right) \sin(2\pi\theta_n) \quad (6)$$

This map is called the circle map. Focus on the region where $K < 1$ and examine the behavior of the system with respect to the parameters Ω and K . Compare this with the return map constructed in the previous exercise and consider the physical correspondence (observe Arnold tongues and the Devil's staircase).

The dependency of the circle map on Ω and K is shown in Fig. (26) left, where the inverted triangular regions represent synchronization. The Devil's staircase corresponding to $K = 1$ is shown in Fig. (26) right.

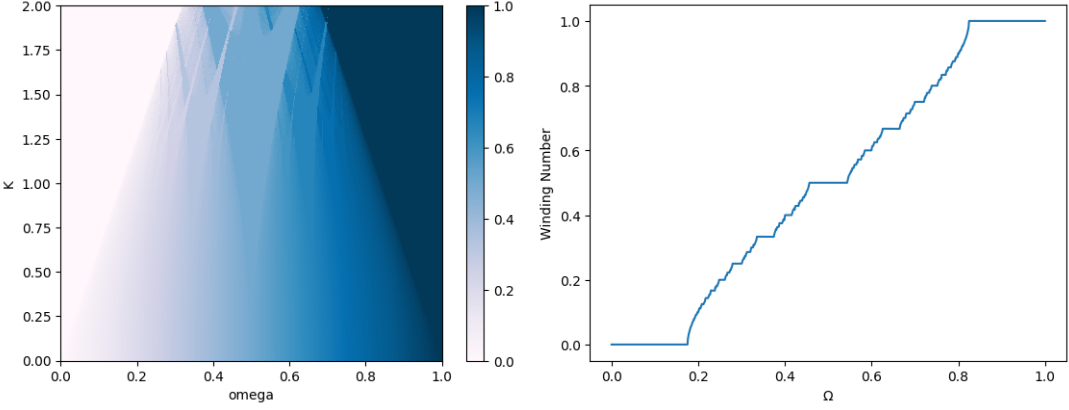


Figure 26: Arnold tongues and Devil's staircase of the circle map

In fact, inverted triangular regions exist at all rational ratios, as seen in Fig. (26) right, indicating that synchronization occurs everywhere in the region where $K < 1$. For example, as shown in Figs. (27)-(29), synchronization occurs everywhere in the regions within Fig. (26) left, and the solution becomes either stable or periodic.

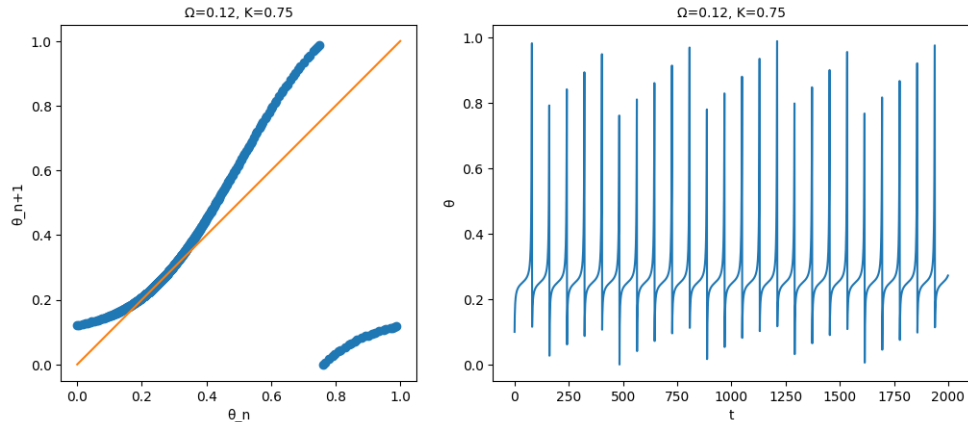


Figure 27: Return map and behavior of θ at $\Omega = 0.12, K = 0.75$

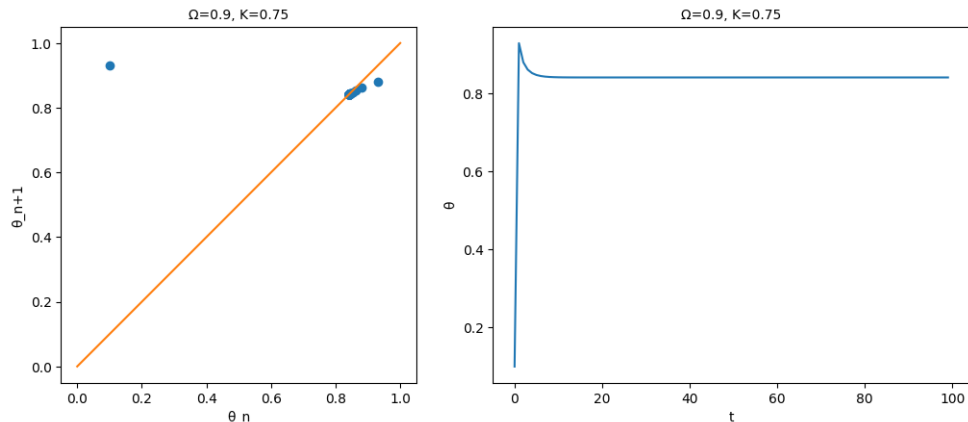


Figure 28: Return map and behavior of θ at $\Omega = 0.9, K = 0.75$

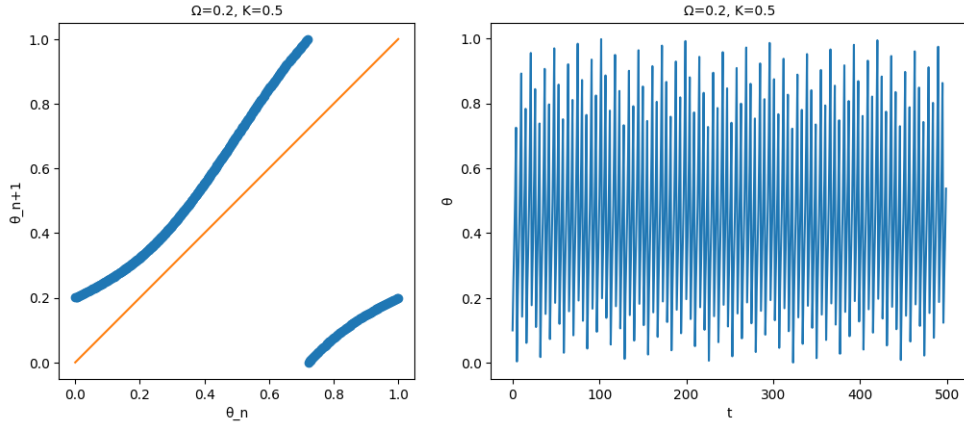


Figure 29: Return map and behavior of θ at $\Omega = 0.2, K = 0.5$

1.3 Neuron Excitation Phenomenon and Hodgkin-Huxley Equations

1.3.1 Exercise 1.3.1

1. Observe properties such as threshold, action potential, and refractory period, as seen in real neurons. Examine how changes in the initial conditions affect the time evolution of membrane potential. Plot the trajectory on the $V - \dot{V}$ plane. How does membrane potential V behave when subjected to a step-like stimulus $I(t)$ at regular intervals?

When $10 < t < 60$, $I = 20mA$ and is 0 otherwise. For the initial values $V = -65mV$, $n = 0.3$, $m = 0.1$, $h = 0.5$, the behavior of membrane potential is shown in Fig. (30). The trajectory of the membrane potential on the $V - \dot{V}$ plane is shown in Fig. (31).

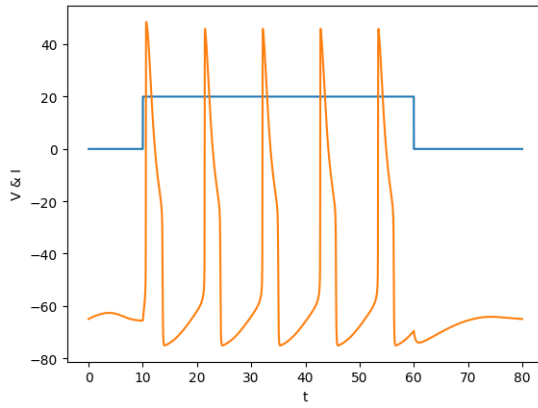


Figure 30: Behavior of membrane potential

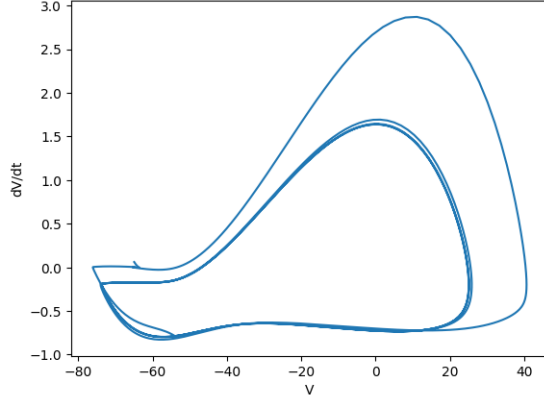


Figure 31: Trajectory of membrane potential (initial values $V = -65mV$, $n = 0.3$, $m = 0.1$, $h = 0.5$)

Furthermore, when the initial conditions are slightly changed, the trajectory of the membrane potential shifts laterally and shows significant changes in shape, as shown in Fig. (32).

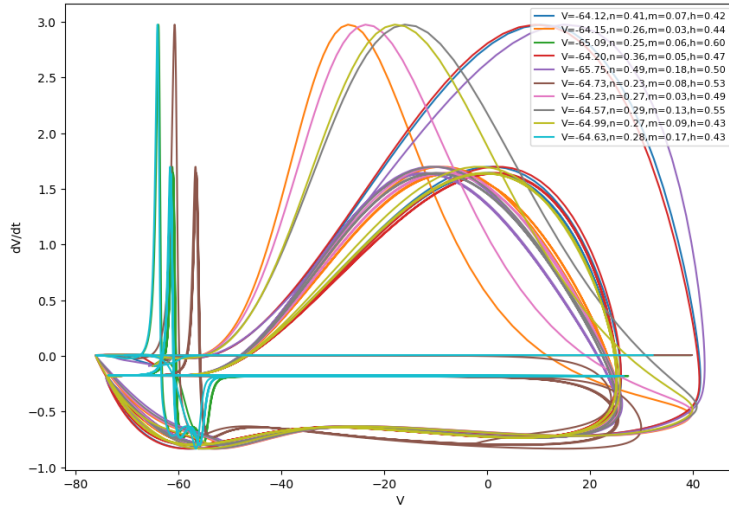


Figure 32: Trajectories of membrane potential under different initial conditions

2. Observe changes in variables other than membrane potential and consider how membrane potential behavior is generated.

Changes in n , m , and h are shown in Fig. (33). From Fig. (33), it is clear that membrane potential V is proportional to n and m and inversely proportional to h . Na^+ channels are controlled by three activation gates (m) and one inactivation gate (h), while K^+ channels are controlled by four activation gates (n). When the potential of activation gates n and m rises and that of inactivation gate h decreases, Na^+ and K^+ flow through the channels, causing the membrane potential to rise. Conversely, when the potential of activation gates n and m decreases and that of inactivation gate h rises, the influx of Na^+ and K^+ slows (or stops), causing the membrane potential to fall. This explains the behavior of membrane potential.

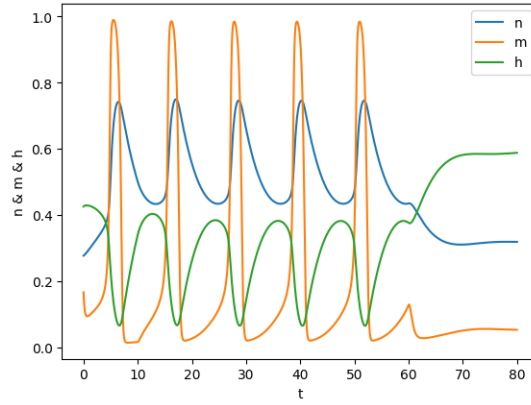


Figure 33: Changes in n , m , and h

3. Examine the range of parameter I where periodic solutions for action potentials can be found.

The bifurcation diagram of action potentials is shown in Fig. (34), with a magnified view in Fig. (35). From the figures, it is clear that resting membrane potential is achieved when $I < 6mA$, while periodic solutions are found when $I > 6.3mA$.

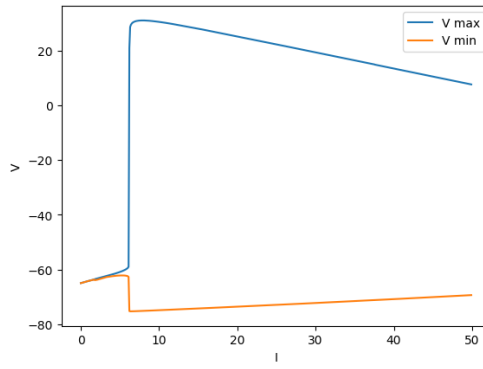


Figure 34: Bifurcation diagram of action potentials

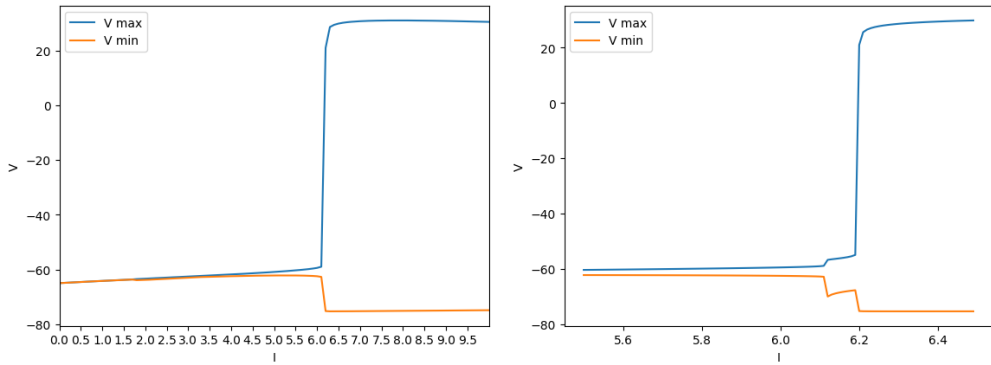


Figure 35: Magnified view of the bifurcation diagram of action potentials

Exercise 1.3.2: Attempt to reduce the 4-variable HH equation to a 2-variable one. To do this, assume that variable m changes much faster than other variables n and h , reaching a steady state immediately. Also, assume that the sum of the slowly changing variables n and h is always constant ($n + h = K(\text{const.})$).

- Evaluate the validity of the two assumptions by observing the behavior of variables V , n , m , and h in the HH equation.

The behavior of V , n , m , and h based on the two assumptions is shown in Fig. (36). Comparing Figs. (30) and (33), the shapes and values of the graphs are similar, and the relationship among n , h , and V is the same as when no assumptions are made, indicating that the assumptions are valid.

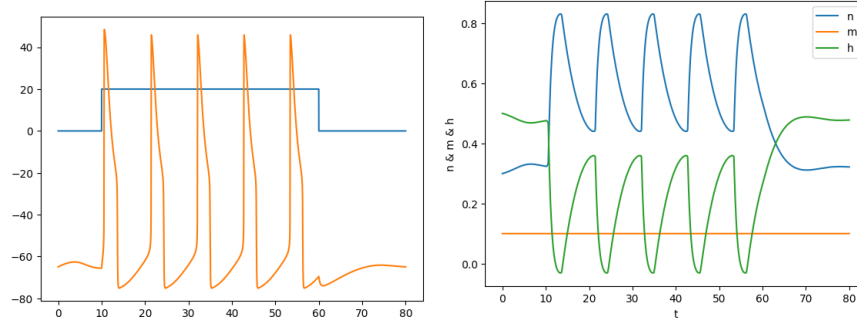


Figure 36: Behavior of V , n , m , and h

- Eliminate m and h using the two assumptions to derive a differential equation for V and n .

$$C_m \frac{dV}{dt} + \bar{g}_K n^4 (V - V_K) + \bar{g}_{Na} \left(\frac{\alpha_m}{\alpha_m + \beta_m} \right)^3 (K - n)(V - V_{Na}) - \bar{g}_L (V - V_L) - I = 0. \quad (7)$$

- Assume $K = 0.75$. Analyze solution trajectories, bifurcation diagrams, etc. Additionally, drawing nullclines is a standard approach for understanding 2-dimensional dynamical systems. How do the nullclines change with bifurcation? It is recommended to use the Newton method when plotting nullclines.

The solution trajectory and bifurcation diagram obtained from the equation in problem 2 are shown in Fig. (37) and Fig. (38), respectively.

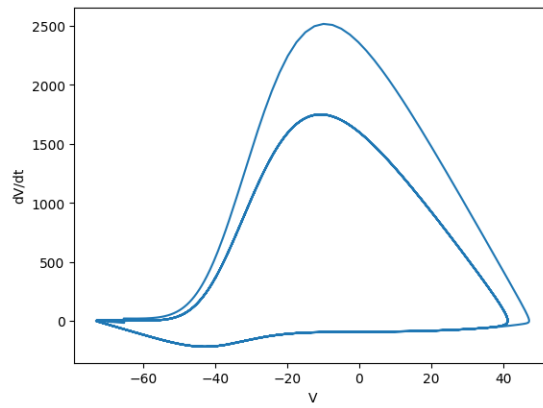


Figure 37: Solution trajectory after eliminating m and h

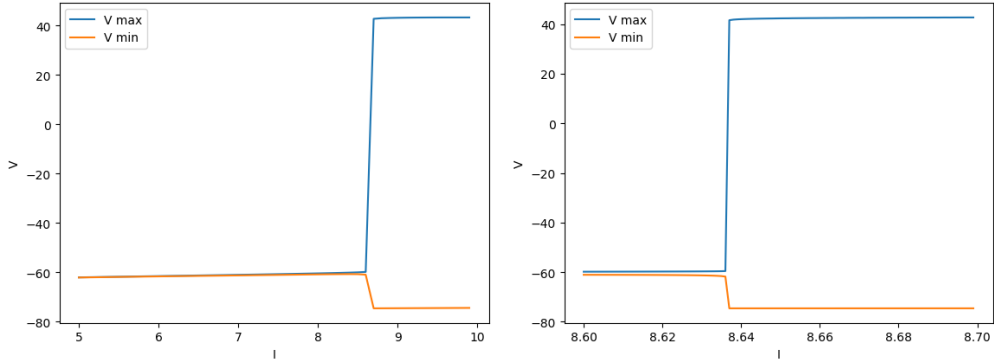


Figure 38: Bifurcation diagram after eliminating m and h

The nullclines are shown in Fig. (39).

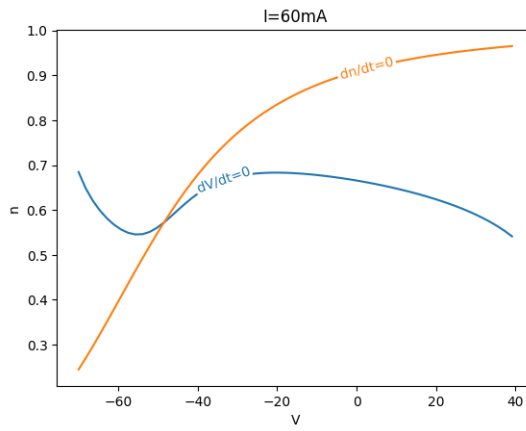


Figure 39: Nullclines for the differential equation of V and n

5. Calculate the FitzHugh-Nagumo equation and examine its nullclines. Compare them with the reduced HH equation.

Assuming $a = b = \tau = I = 1$, the nullclines of the FitzHugh-Nagumo equation are shown in Fig. (40), which are similar to those of the reduced HH equation. This indicates that the dynamics of both solution trajectories are similar.

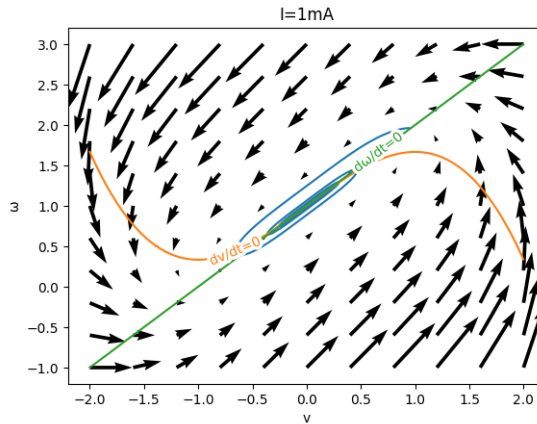


Figure 40: Nullclines of the FitzHugh-Nagumo equation

1.4 Chaos

1.4.0 Exercise 1.4.0

1. Observe the time series and trajectories of the following systems.

The phase space of the Henon map with $a = 1.4, b = 0.3$ is shown in Fig. (41), where zooming in on certain parts confirms the fractal nature of the attractor.

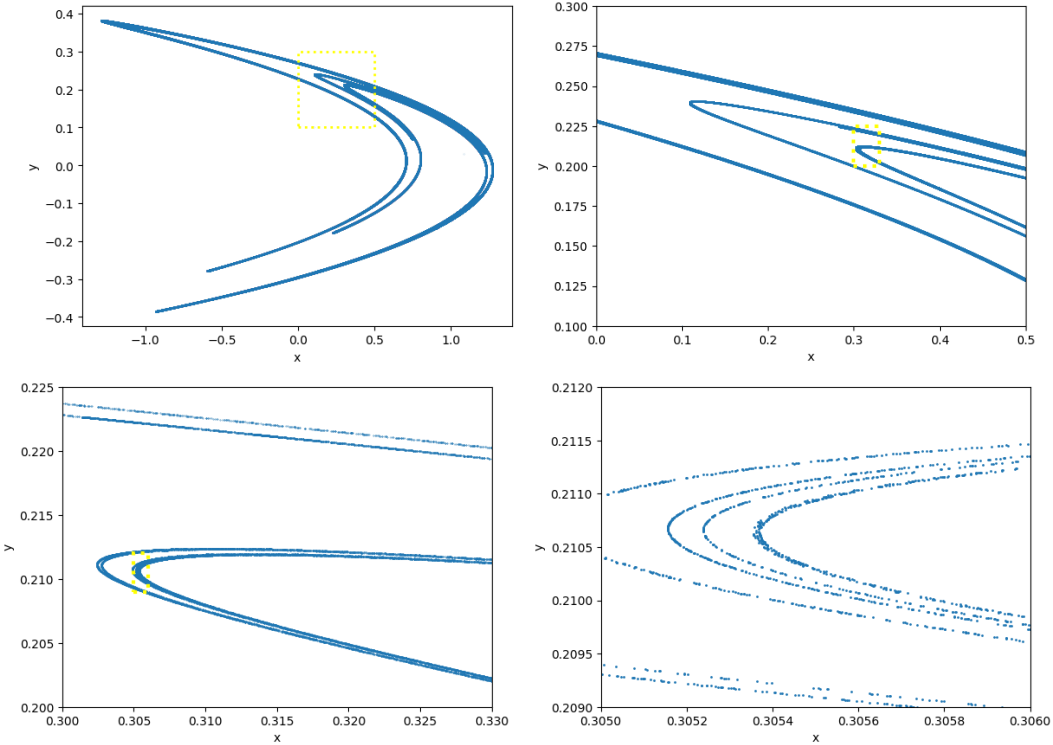


Figure 41: Phase space of the Henon map

The trajectory of the Lorenz system with $\sigma = 10, r = 28, b = \frac{8}{3}$ is shown in Fig. (42).

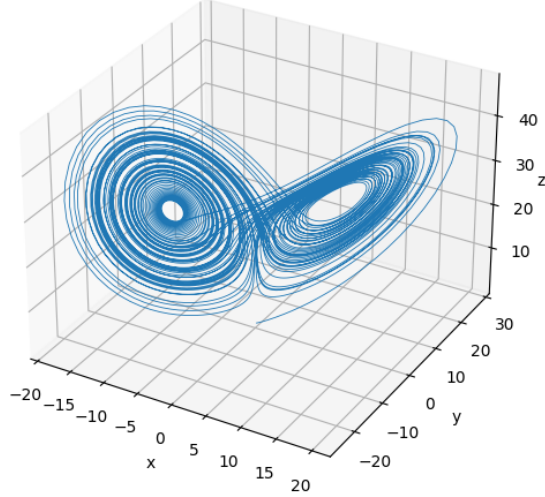


Figure 42: Trajectory of the Lorenz system

The trajectory of the Rossler system with $a = b = 0.2, c = 5.7$ is shown in Fig. (43).

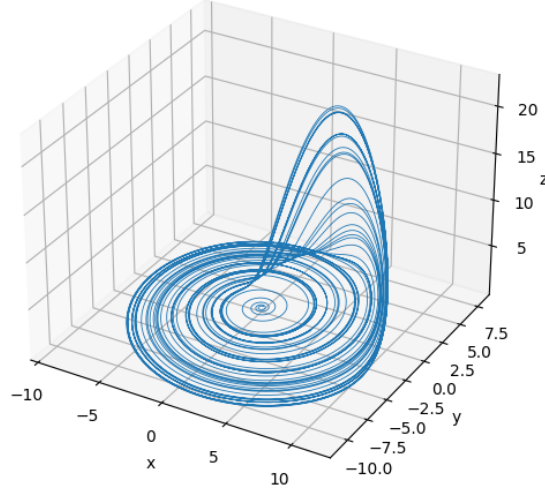


Figure 43: Trajectory of the Rossler system

2. Examine the time evolution of the distance (in phase space) between two trajectories with slightly different initial conditions.

In the Lorenz system, setting the initial values (x, y, z) as $(1, 1.2, 1.3)$ and $(0.8, 1.5, 1.4)$, the time evolution of the distance between the two trajectories is shown in Fig. (44). The vertical axis represents the logarithm of the distance.

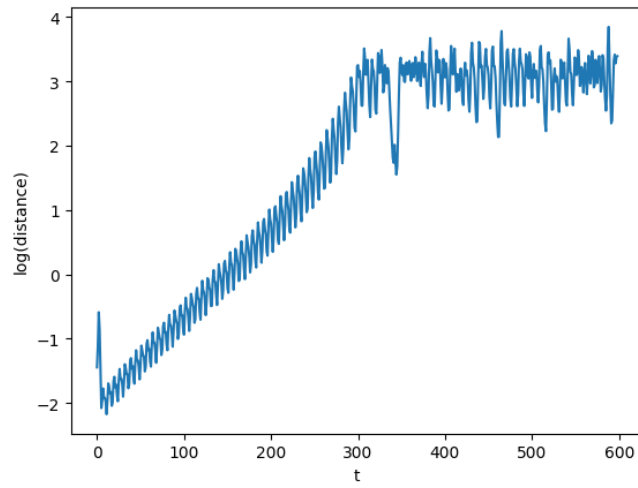


Figure 44: Time evolution of the distance between two trajectories in the Lorenz system

3. Take many initial conditions within a small region and observe the time evolution of their distribution.

Setting 100 points uniformly distributed over a 0.1×0.1 square as the initial values, the time evolution of the Henon map trajectories is shown in Fig. (45).

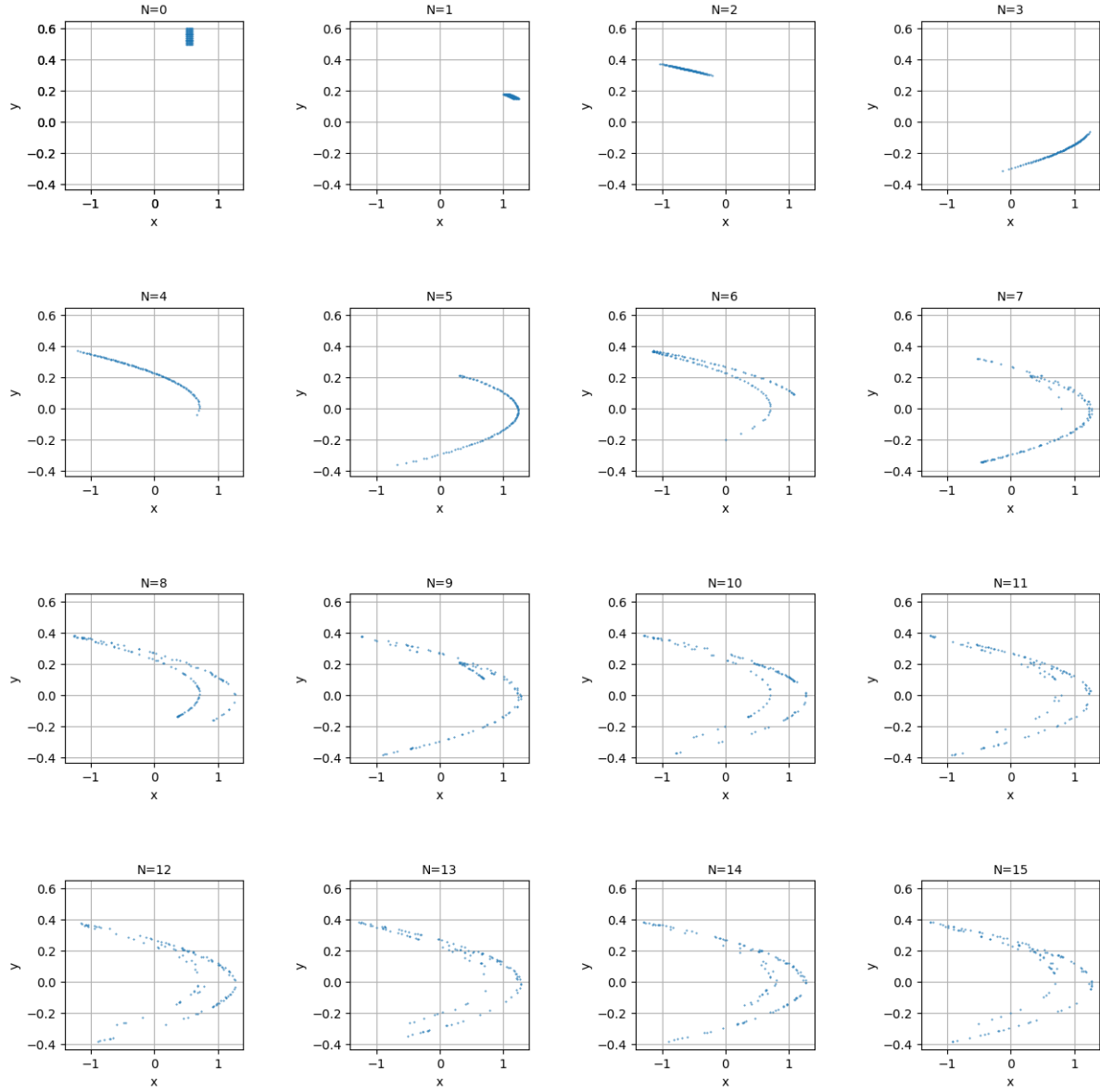


Figure 45: Time evolution of the Hénon map

Setting 1000 points uniformly distributed within a $0.1 \times 0.1 \times 0.1$ cube as the initial values, the time evolution of the Lorenz system trajectories is shown in Fig. (46).

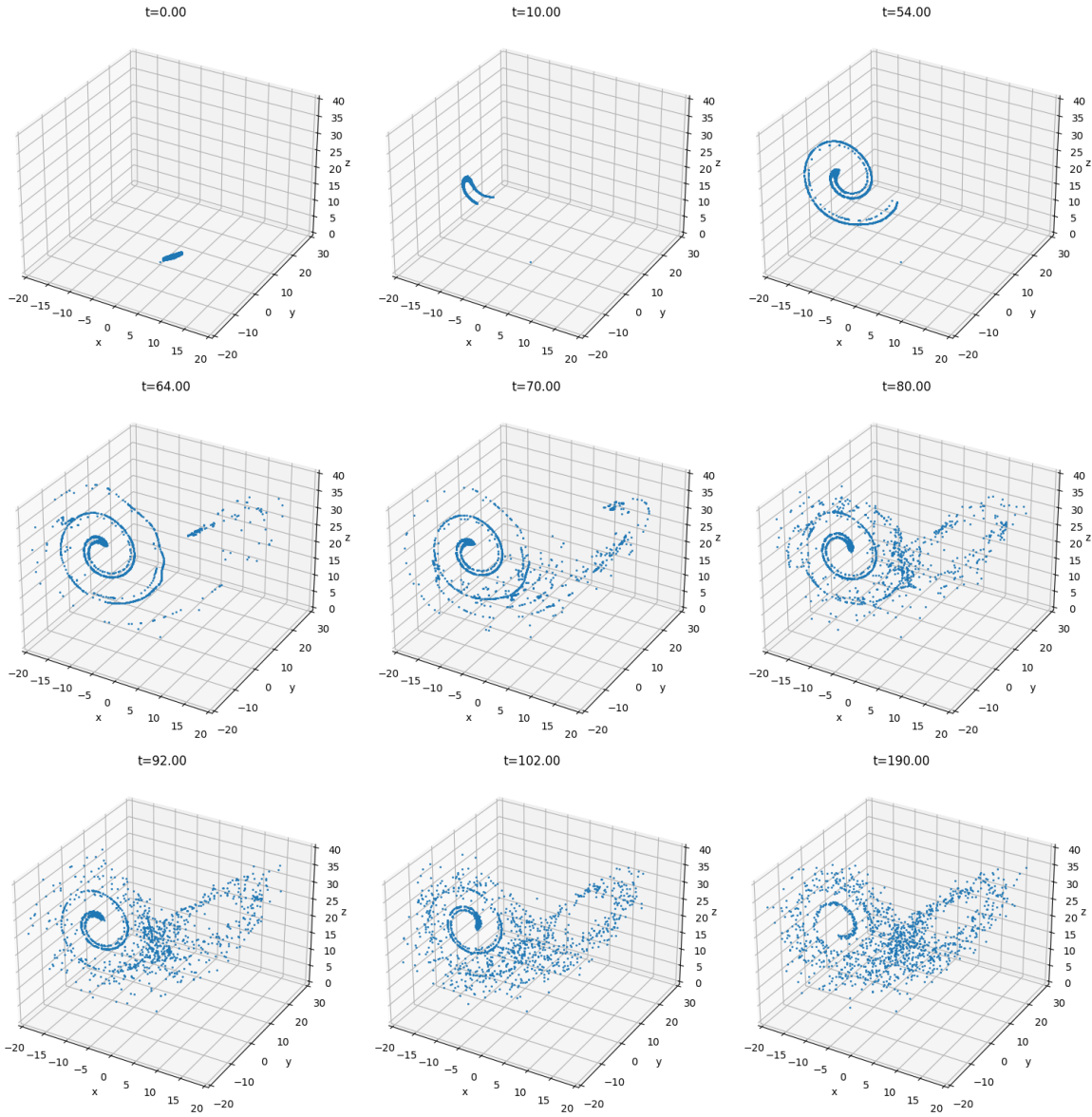


Figure 46: Time evolution of the Lorenz system

Setting 1000 points uniformly distributed within a $0.1 \times 0.1 \times 0.1$ cube as the initial values, the time evolution of the Rossler system trajectories is shown in Fig. (47).

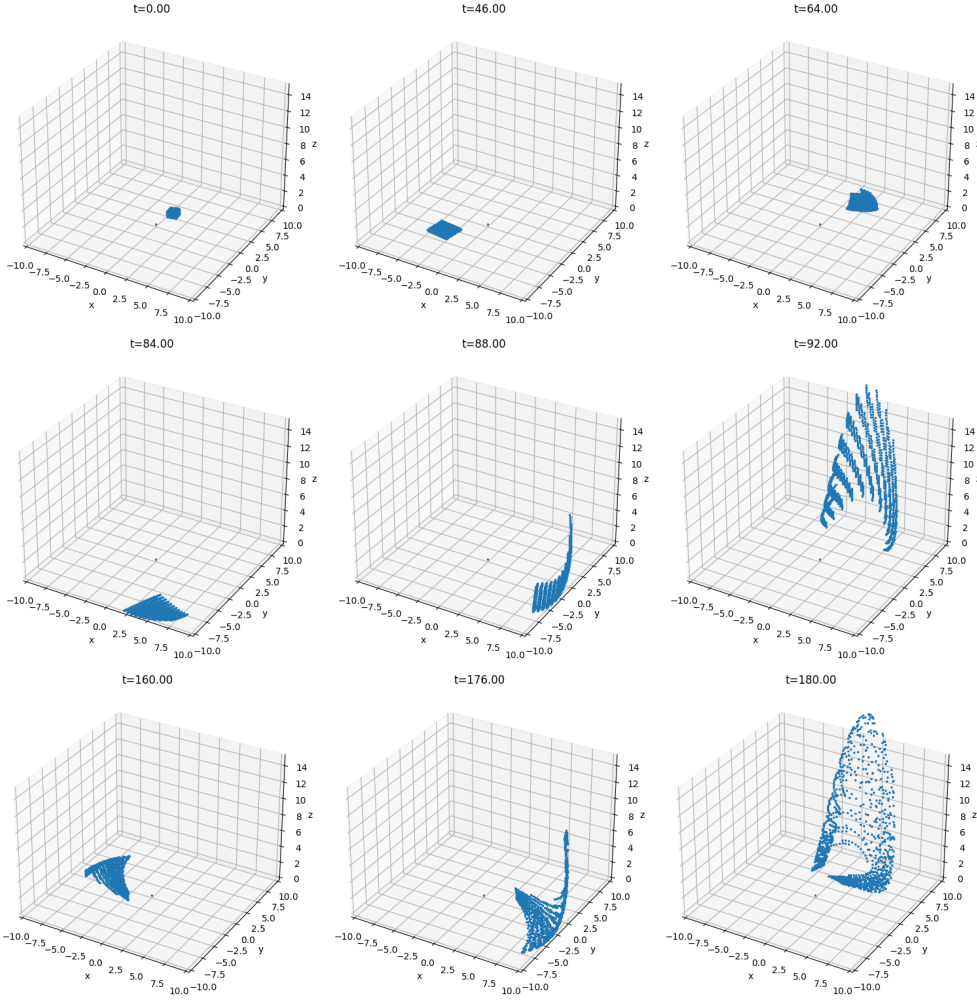


Figure 47: Time evolution of the Rossler system

From these results, it is evident that in chaos, the area (or volume) of a small region of initial conditions expands over time, changing the shape of the region. This represents the sensitive dependence on initial conditions, a characteristic of chaos.

Characterization of Chaos

1.4.1 Exercise 1.4.1

- For the three models mentioned earlier, analytically calculate the rate of decrease of phase space volume and verify the results with numerical calculations.

The determinant of the Jacobian matrix of the Henon map represents the rate of change of volume in phase space after one mapping. The determinant of this map's Jacobian is $-b$, and in this case, $b = 0.3$ implies that the rate of decrease of phase space volume (area) is 0.3.

In the Lorenz and Rossler equations, let $\dot{x}, \dot{y}, \dot{z}$ be

$$\dot{x} = f(x, y, z), \quad \dot{y} = g(x, y, z), \quad \dot{z} = h(x, y, z). \quad (8)$$

Considering a cube around point (x, y, z) with edges $\delta x, \delta y, \delta z$, after time dt , point (x, y, z) will move to $(x + f(x, y, z)dt, y + g(x, y, z)dt, z + h(x, y, z)dt)$. Also, after time dt , the x coordinate of $(x + \delta x, y + \delta y, z + \delta z)$ will be $x + \delta x + f(x + \delta x, y, z)dt$. Hence, the edge in the x direction will extend from δx to

$$\delta x + [f(x + \delta x, y, z) - f(x, y, z)]dt = \delta x(1 + \frac{\partial f(x, y, z)}{\partial x}dt). \quad (9)$$

The calculations for the y and z directions are similar. The volume $V = \delta x \delta y \delta z$ will change after time dt as

$$(1 + \frac{\partial f(x, y, z)}{\partial x} dt)(1 + \frac{\partial g(x, y, z)}{\partial y} dt)(1 + \frac{\partial h(x, y, z)}{\partial z} dt)V = (1 + [\frac{\partial f(x, y, z)}{\partial x} + \frac{\partial g(x, y, z)}{\partial y} + \frac{\partial h(x, y, z)}{\partial z}]dt)V, \quad (10)$$

leading to the volume increment

$$dV = (\frac{\partial f(x, y, z)}{\partial x} + \frac{\partial g(x, y, z)}{\partial y} + \frac{\partial h(x, y, z)}{\partial z})V dt. \quad (11)$$

Thus,

$$\frac{dV}{dt} = (\frac{\partial f(x, y, z)}{\partial x} + \frac{\partial g(x, y, z)}{\partial y} + \frac{\partial h(x, y, z)}{\partial z})V. \quad (12)$$

Applying the above equation to the Lorenz system yields:

$$\frac{dV}{dt} = -(1 + \sigma + b)V. \quad (13)$$

Thus, $V(t) = V(0)e^{-(1+\sigma+b)t}$. Setting $V(0) = 10^{-3}, \sigma = 10, b = \frac{8}{3}$ gives $V(t) = 10^{-3}e^{-\frac{41}{3}t}$. Therefore, the rate of decrease of phase space volume is $\frac{41}{3000e^{\frac{41}{3}}}$.

For the Rossler equation, applying the above equation gives:

$$\frac{dV}{dt} = (x + a - c)V. \quad (14)$$

Since x is included, we take a specific numerical value for calculation. For instance, with an initial value of $x = 0.1$, we obtain $V(t) = V(0)e^{(0.1+a-c)t}$. Setting $V(0) = 10^{-3}, a = 0.2, c = 5.7$ gives $V(t) = 10^{-3}e^{-5.4t}$. Therefore, the rate of decrease of phase space volume is $\frac{54}{10000e^{5.4}}$.

2. Calculate the box-counting dimension (capacity dimension), information dimension, and correlation dimension for the Henon map.

According to

$$D_0 = \lim_{\epsilon \rightarrow 0} \frac{\log \tilde{N}(\epsilon)}{\log(\frac{1}{\epsilon})}, \quad (15)$$

setting $\epsilon = 0.001$, the calculated box-counting dimension is $D_0 \approx 1.29$, which is close to the theoretical value $D_0 \approx 1.27$, indicating that the calculation is reasonable.

Moreover,

$$D_1 = \lim_{\epsilon \rightarrow 0} \frac{I(\epsilon)}{\log(\frac{1}{\epsilon})}, \quad I(\epsilon) = -\sum_{i=1}^{\tilde{N}(\epsilon)} p_i \log p_i, \quad p_i = \frac{N_i}{N}, \quad (16)$$

calculated with $\epsilon = 0.01$ gives the information dimension of the Henon map as $D_1 \approx 1.503$.

Furthermore,

$$D_2 = \lim_{\epsilon \rightarrow 0} \frac{\log(\sum_{i=1}^{\tilde{N}(\epsilon)} p_i^2)}{\log(\epsilon)}, \quad (17)$$

calculations yield the correlation dimension of the Henon map as $D_2 \approx 1.45$ for $\epsilon = 0.01$, $D_2 \approx 1.35$ for $\epsilon = 0.003$, and $D_2 \approx 1.25$ for $\epsilon = 0.001$. Therefore, as ϵ decreases, the correlation dimension approaches the theoretical value of 1.23.

3. For the logistic map

$$x_{n+1} = ax_n(1 - x_n), \quad (18)$$

observe the trajectory while varying the parameter ($0 < a < 4$). How does the distance between trajectories with slightly different initial conditions change for each parameter?

The trajectories for $a = 0.7, 2.5, 2.8, 3.5$ and the distances between two trajectories with initial values of 0.1 and 0.2 are shown in Figures 48-51. The figures indicate that for small a , x_n stabilizes over time, but as a increases, it takes longer for x_n to stabilize. For even larger a , x_n becomes unstable and

exhibits periodic solutions. Moreover, the distances between the two trajectories with initial values of 0.1 and 0.2 converge to zero in all four cases (i.e., $a = 0.7, 2.5, 2.8, 3.5$), suggesting that sensitivity to initial conditions is not very high. However, for $a = 3.5$, if the initial values are set to 0.1 and 0.21, the distance between the two trajectories does not converge to zero and becomes periodic (Figure 52). This indicates that the logistic map becomes highly sensitive to initial conditions for large a .

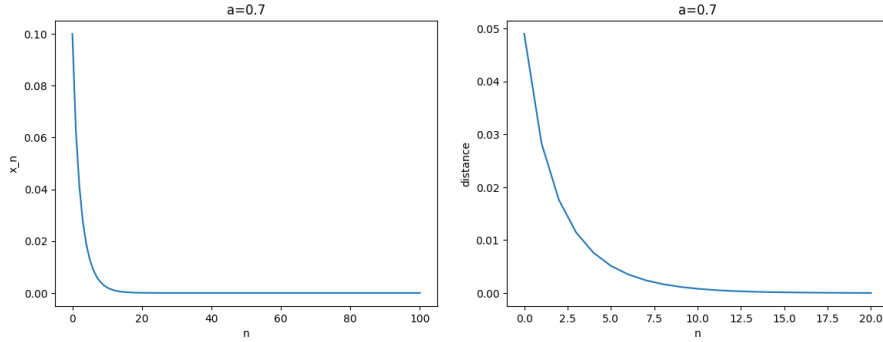


Figure 48: Logistic map for $a = 0.7$ (left) and distance between trajectories with slightly different initial conditions (right)

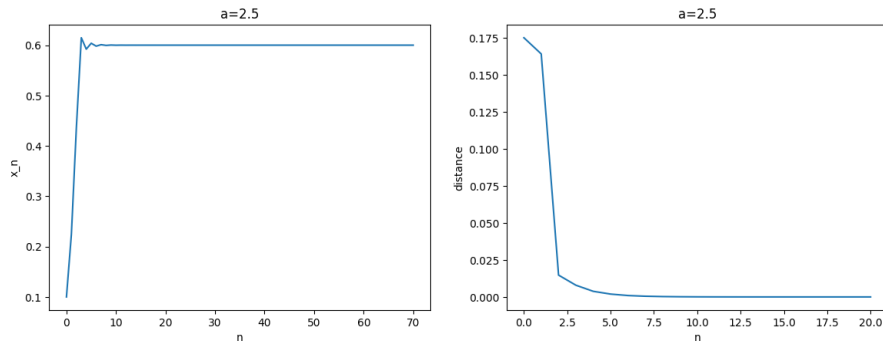


Figure 49: Logistic map for $a = 2.5$ (left) and distance between trajectories with slightly different initial conditions (right)

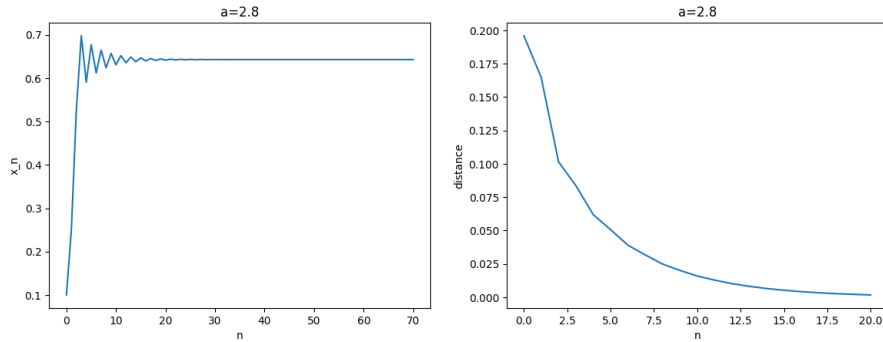


Figure 50: Logistic map for $a = 2.8$ (left) and distance between trajectories with slightly different initial conditions (right)

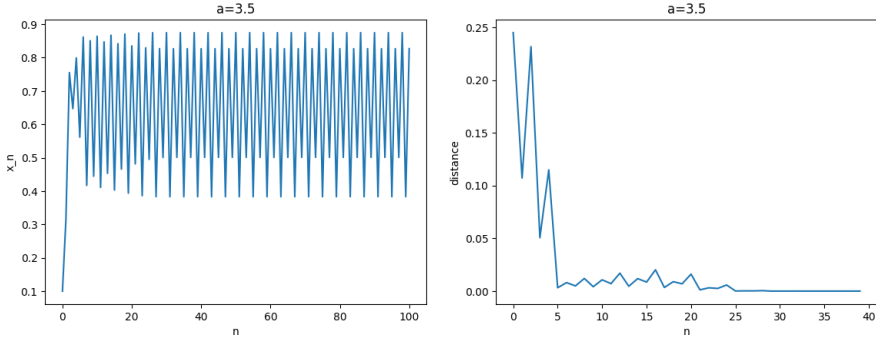


Figure 51: Logistic map for $a = 3.5$ (left) and distance between trajectories with slightly different initial conditions (right)

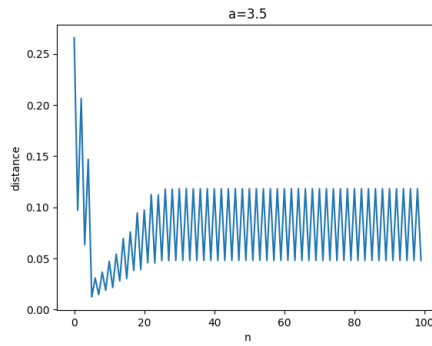


Figure 52: Distance between two trajectories with initial values of 0.1 and 0.21 for $a = 3.5$

4. For the Rossler system, take the Poincaré section at $x < 0, y = 0$ and construct the return map. Compare the results with the logistic map. How does the stretching and folding structure of the Rossler attractor reflect in the properties of the map?

The return maps for x and z in the Poincaré section at $x < 0, y = 0$ are shown in Figure 53, and both have shapes resembling quadratic functions. Meanwhile, the logistic map is given by $x_{n+1} = ax_n(1 - x_n)$, so defining $f(x) = -ax^2 + ax$, it becomes evident that the return map of the logistic map corresponds to a quadratic shape. This indicates that the return maps for x and z in the Rossler system align with the shape of the logistic map's return map. Additionally, when a is large, the solution of the logistic map becomes unstable and periodic, which corresponds to the solution trajectory of the Rossler system, where the solution becomes unstable and exhibits periodic behavior over time. This explains the stretching and folding structure observed in the Rossler system.

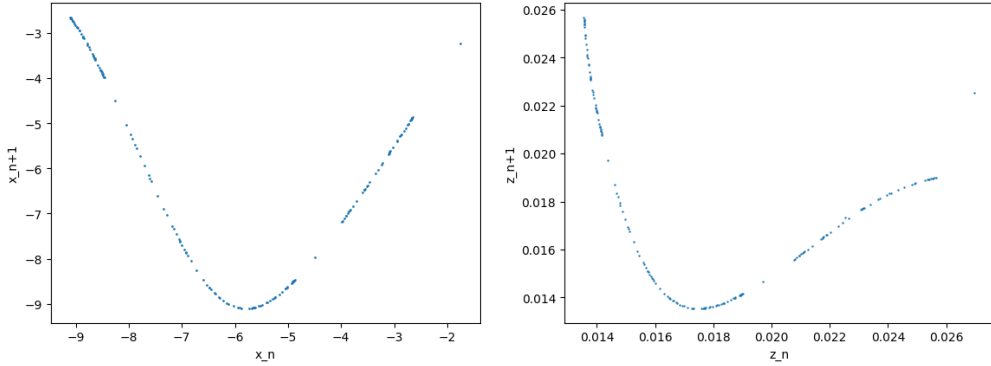


Figure 53: Return maps for x (left) and z (right)

5. Draw the bifurcation diagrams for the logistic map and the Rossler system. (For the Rossler system, examine the region where $c^2 > 4ab$.) What similarities do they share?

The bifurcation diagram for the logistic map is shown on the left in Figure 54, and the bifurcation diagram for the Rossler system with respect to b when $a = 0.2, c = 5.7$ is shown on the right. As the figures show, the logistic map becomes periodic and then chaotic as a increases, whereas the Rossler system exhibits the opposite behavior: as b increases, the solution transitions from chaos to periodic behavior and then to stability. Thus, both systems share the characteristic of transitioning from stability to periodic behavior and then to chaos, but this progression occurs with increasing a for the logistic map, while it occurs with decreasing b for the Rossler system.

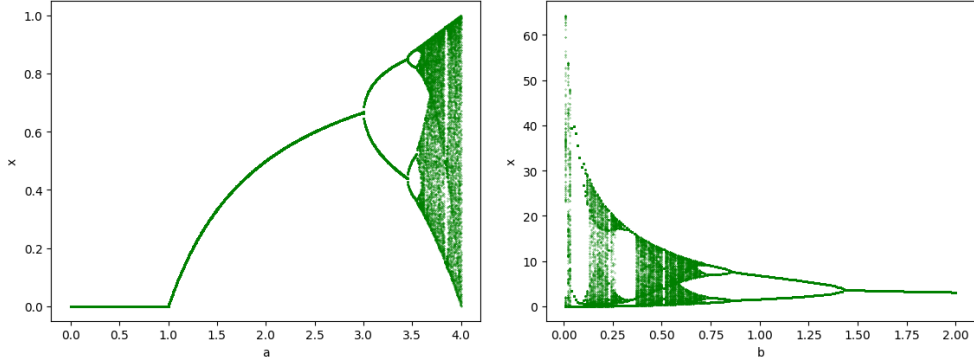


Figure 54: Bifurcation diagrams for the logistic map (left) and the Rossler system (right)

6. Calculate the Lyapunov exponent for the logistic map and compare it with the bifurcation diagram.

The Lyapunov exponent for the logistic map is shown in Figure 55. The figure indicates that the Lyapunov exponent becomes positive when the logistic map exhibits chaos, which signifies that a positive Lyapunov exponent implies exponential divergence of nearby trajectories, indicating the presence of chaos.

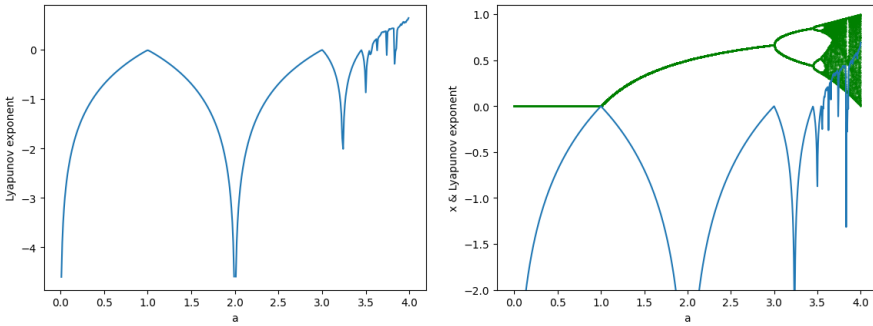


Figure 55: Correspondence between the Lyapunov exponent and the bifurcation diagram for the logistic map

7. Investigate the power spectrum of the Rossler system. How does it change depending on the parameter c ? Compare it with the bifurcation diagram.

The power spectrum for the four values of b shown in Figure 56 is presented in Figure 57. As seen in the figures, when the solution exhibits chaos, the frequency is disordered; as it becomes periodic and eventually stable, the frequency becomes gradually more regular. In other words, as the solution becomes periodic and eventually stable, only lower frequencies appear in the power spectrum.

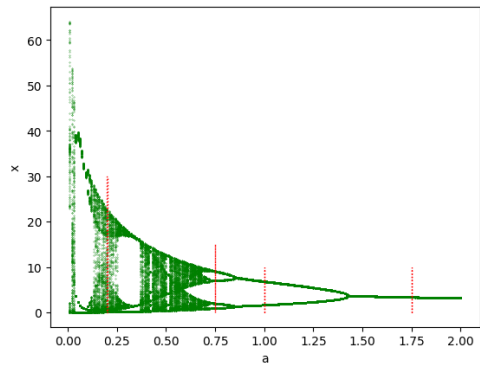


Figure 56: Values of b taken for analysis

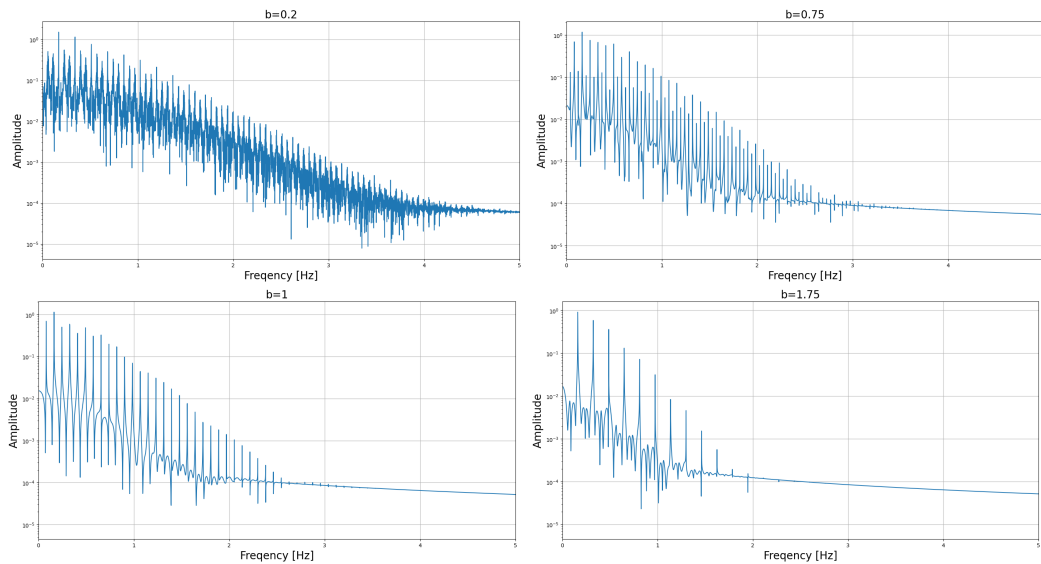


Figure 57: Power spectrum of the Rossler system for $b = 0.2$ (top left), 0.75 (top right), 1 (bottom left), and 1.75 (bottom right)